Article

Synthesis of Xanthohumol Analogues and Discovery of Potent Thioredoxin Reductase Inhibitor as Potential Anticancer Agent

Baoxin Zhang, Dongzhu Duan, Chunpo Ge, Juan Yao, Yaping Liu, Xinming Li, and Jianguo Fang

Just Accepted

Synthesis of Xanthohumol Analogues and Discovery of Potent Thioredoxin Reductase Inhibitor as Potential Anticancer Agent

Baoxin Zhang, Dongzhu Duan, Chunpo Ge, Juan Yao, Yaping Liu, Xinming Li, Jianguo Fang*

State Key Laboratory of Applied Organic Chemistry and College of Chemistry and Chemical

Engineering, Lanzhou University, Lanzhou 730000, China

*Corresponding author, E-mail: fangjg@lzu.edu.cn (J. Fang); Fax: +86 931 8915557.

ABSTRACT

The selenoprotein thioredoxin reductases (TrxRs) are attractive targets for anticancer drugs

development. Xanthohumol (Xn), a naturally occurring polyphenol chalcone from hops, has

received increasing attention due to its multiple pharmacological activities. We synthesized Xn

and its 43 analogues, and discovered compound **13n** displayed the highest cytotoxicity towards

HeLa cells (IC_{50}=1.4 μM). Structure-activity relationship study indicates that the prenyl group is

not necessary for the cytotoxicity, and introducing electron-withdrawing group, especially on the

meta-position, is favored. In addition, methylation of the phenoxyl groups generally improves the

potency. Mechanistic study revealed that **13n** selectively inhibits TrxR, induces reactive oxygen

species and apoptosis in HeLa cells. Cells overexpressing TrxR are resistant to **13n** insult, while

knockdown of TrxR sensitizes cells to **13n** treatment, highlighting the physiological significance

of targeting TrxR by **13n**. The clarification of the structural determinants for the potency would

guide the design of novel potent molecules for future development.

1

INTRODUCTION

The thioredoxin system, composed of thioredoxin reductase (TrxR), thioredoxin (Trx), and

NADPH, is a highly conserved, ubiquitous network in all cells, and plays crucial roles in the

redox regulation of numerous cellular signaling pathways involved in cell survival and

proliferation.[1-3] Reduced Trx carries on the principal function of the system via a reversible

thiol-disulfide exchange reaction during transfer of reducing equivalents to various cellular targets

to generate an oxidized form of Trx, which is in turn recycled to a reduced state by taking

electrons from NADPH under TrxR catalysis. As TrxR is the only known physiological enzyme

to catalyze the reduction of oxidized Trx, the function of the thioredoxin system is strictly

controlled by the activity of TrxR. Mammalian TrxRs, compared to those from bacteria, are large

selenium-containing proteins with a penultimate selenocysteine (Sec) in the C-terminal active

site.[4, 5] This flexible C-terminal extension enables TrxR to extend the electron transport chain

from the catalytic disulfide to the enzyme surface. Mammalian TrxRs have a broad range of

substrates and are easily inactivated by various alkylating agents[6, 7] presumably due to the

presence and easy accessibility of the high reactive Sec residue in the reduced form of the

enzymes. In recent years, accumulating evidence supports that TrxR is a promising target for

development of novel anticancer agents as the thioredoxin system is often overexpressed in many

tumors,[8, 9] and this overexpression confers drug resistance in cancer chemotherapy.[10] The

physiological importance of TrxR for tumor progression was demonstrated by Hatfield *et al.*,

showing that knockdown of TrxR prevents tumor formation, and inhibits self-sufficient growth

and DNA replication of cancer cells.[11, 12] Thus, the past years have witnessed a great endeavor in

discovering and developing a variety of TrxR-targeted small molecules as potential therapeutic

agents.[6, 13-22]

Natural products and their derivatives are invaluable fountain of therapeutic agents, and have driven pharmaceutical discovery over the past century. The diversity of natural products continue to provide a unique source of bioactive lead compounds for drug development.[23, 24] It is roughly estimated that half of modern marketed drugs are natural products or their derivatives. In the case of anticancer and anti-infective agents, this proportion is even higher.[23, 25] As essence of the drug discovery progress, generation of novel and structurally diverse molecules with potential biological properties has been actively pursued. Chalcones, also known as α, β-unsaturated ketones, form a central core of various natural products, such as flavokawain, butein, licochalcone, xanthoangelol, xanthohumol, derricin, cardamonin, isoliquiritigenin, isosalipurposide, and naringenin. The chalcones family has been documented with diverse biological function, including immunomodulation, anti-inflammation, anticancer, and antidiabetic activity, and some of them have been approved for clinical application or tested in humans.[26, 27] Xanthohumol, a structurally simple prenylated chalcone, is the major prenylflavonoid that is extracted from the hop plant, *Humulus lupulus,* which is widely used in beers and a few types of soft drinks, such as Julmust and Malta. The presence of high concentration of Xn in beers has been suggested to link to the epidemiological observation of the beneficial effect of regular beer drinking.[28] Xanthohumol has been characterized as a 'broadspectrum' anticancer agent,[29] and some putative mechanisms underlying the effect of Xn have been reported, including generation of ROS,[30-32] downregulation of anti-apoptotic proteins,[33-36] upregulation of p53,[37, 38] and induction of phase II enzymes.[39, 40] Despite the well-documented anticancer activity of Xn, its efficacy is moderate, and hence it is of demand to improve the potency of Xn for future development.

3

As our continuous interests in discovering and developing small molecule regulators of cellular redox system as potential therapeutic agents,[6, 15, 41-47] we synthesized a series of Xn analogues, and evaluated their cytotoxicity in different types of cancer cells. In the cultured HeLa cells, compound **13n** displayed the greatest potency with an IC_{50} value of 1.4 µM, more than 30-fold increase compared to the lead compound Xn. Further mechanistic studies disclose that **13n** may selectively inhibit TrxR by primarily targeting the Sec residue in the antioxidant enzyme, leading to the accumulation of ROS. As a consequence, **13n** elicits oxidative stress, and eventually induces apoptosis in HeLa cells. Importantly, overexpression of the functional TrxR in cells alleviates the cytotoxicity of **13n**, while knockdown of the enzyme augments the cytotoxicity, supporting the physiological significance of targeting TrxR by **13n**.

RESULTS AND DISCUSSION

Chemistry. Analysis of the chemical structure of Xn reveals it belongs to the chalcones family, the structure of which could be easily constructed by the base-catalyzed Claisen-Schmidt condensation of an aldehyde with a ketone in a polar solvent like ethanol or methanol. Numerous bases have been applied in the condensation reaction, including NaOH, KOH, Ba(OH)$_2$, and LiHMDS, which were summarized in the recent publication.[48] We employed KOH as a catalyst in anhydrous methanol for the construction of the skeleton of all chalcone derivatives used in the present study (Schemes 1-3).[49, 50] In brief, the different substituted acetophenone was dissolved in anhydrous methanol followed by addition of a catalytic amount of KOH. The reaction mixture was stirred at room temperature for an appropriate time followed by the addition of diverse substituted benzaldehyde. The reaction was carried out at room temperature until completion, and

the corresponding chalcone derivative (**8a-8n**, **11a-11n**, and **13a-13q**) was isolated by crystallization or by silica gel flash chromatography. For the synthesis of Xn and its prenylated chalcone derivatives, insertion of a prenyl group onto the aryl ring was achieved by a para-Claisen rearrangement after using a Mitsunobu reaction to establish the key prenyl ether precursor (**4**). A Claisen–Schmidt condensation was deployed to construct the chalcone scaffold followed by removal of methoxymethyl (MOM) protecting groups under acidic conditions that were optimized to prevent concomitant cyclization to the flavone. All chalcone derivatives were fully characterized by ^{1}H, ^{13}C NMR, and MS. The purity of all chalcones was determined by HPLC analysis, and was greater than 95%.

Cytotoxicity of Xn and its analogues. Initially, we adopted the MTT assay to screen the cytotoxicity of all compounds (**8a-8m**, **11a-11n**, and **13a-13q**) towards three different types of cancer cell lines. Under this condition, the concentrations that inhibit the cell proliferation to 50% of the control (IC$_{50}$ values) were summarized in Tables 1-3. Several compounds showed promising cytotoxicity, such as **8l**, **11n**, **13m**, **13n**, and **13o**. Next, we chose these five compounds for further follow-up studies. As listed in Table 4, compound **13n** is the most potent one among all the tested compounds with the highest potency towards HeLa cells (IC$_{50}$=1.4 μM). To confirm the results from the MTT assay, we also employed the trypan blue exclusion assay to determine the cell viability upon treatment of HeLa cells with varying concentrations of **13n**, which gives an IC$_{50}$ value of 1.7 μM, quite consistent with the value from the MTT assay. Compared to Xn (IC$_{50}$>40 μM for HeLa cells), the cytotoxicity of **13n** was greatly improved.

Inhibition of TrxR by 13n in vitro and in cells. Since **13n** displays the highest cytotoxicity to HeLa cells, we then asked the possible cellular target of the compound. The core feature of

chalcones is that they contain an α, β-unsaturated keton moiety, a key structure for many reported

TrxR inhibitors.[43-45, 51-54] Thus we speculated that **13n** might be a novel inhibitor of TrxR. As

shown in Fig. 1A, **13n** gave a clear inhibition of TrxR with an IC_{50} value around 12.8 μM (line

with closed squares). As many TrxR inhibitors have been demonstrated to target the Sec residue

in the enzyme, we further determined the inhibition of **13n** towards the mutant enzyme, U498C

TrxR, where the Sec498 was replaced by Cys. Compared to the wild type TrxR, **13n** gave very

weak inhibition to U498C TrxR (line with open circles), suggesting that targeting the Sec residue

is involved in the inhibition of TrxR. Glutathione reductase (GR) is a homologous of TrxR with

similar overall structure. Again, **13n** had marginal effect on the enzyme activity (line with closed

triangles). We also determined the possible inhibition of glutathione peroxidase (GPx), a

Sec-containing enzyme, by **13n**, and no apparent inhibition of the GPx was observed (line with

open inverted triangles). Taken together, **13n** selectively targets the Sec residue in TrxR to inhibit

its activity in vitro. We also evaluated the inhibition of TrxR by Xn, **8l**, **11n**, **13m**, and **13o**. As

shown in Fig. S1 in the Supporting Information (SI), all the tested compounds are inhibitors of

TrxR, while compound **13n** gives the most potent inhibition. Next, we determined the TrxR

activity in HeLa cells after **13n** treatment. Two different assays, *i. e.*, the classic Trx-mediated

insulin reduction assay developed by Holmgren[55] and the fluorogenic probe

(TRFS-green)-based live cell imaging assay developed by our group,[41] were employed. Both

assays gave consistent results and displayed clear concentration-dependent inhibition of TrxR by

13n in HeLa cells (Fig. 1B & C). The IC_{50} value of 3.5 μM could be obtained from the

Trx-mediated insulin reduction assay. Compound to the lead compound Xn (IC_{50}>40 μM, Fig.

1B), the inhibition of cellular TrxR by **13n** was much improved. One of the functions of the

6

thioredoxin system is to prevent the oxidation of cellular thiols, especially the protein thiols. As a

consequence of inhibition of TrxR by **13n**, the cellular thiols decreased remarkably after **13n**

treatment (Fig. S2 in SI).

Induction of ROS in cells by 13n. One of the outstanding functions of the Trx system is to

maintain the intracellular redox homeostasis and defend against oxidative stress. Besides its direct

counteraction of ROS, TrxR is the only known enzyme in maintaining reduced Trx pools for

ribonucleotide reductase in DNA synthesis,[56] and many antioxidant enzymes such as

peroxiredoxins[57] and methionine sulfoxide reductases[58] under physiological conditions. Inhibition

of TrxR would be expected to disturb the cellular redox balance and cause accumulation of ROS

in cells. DCFH-DA is a well-established probe to detect intracellular production of ROS. After

uptaken by cells, DCFH-DA is hydrolyzed by cellular esterases to dichlorodihydrofluorescin

(DCFH), which is trapped within the cell. The nonfluorescent DCFH is then oxidized to

fluorescent dichlorofluorescin by action of cellular ROS. As shown in Fig. 2, the ROS level in

HeLa cells is undetectable under basal conditions. Upon treatment of the cells with **13n**, a

remarkable elevation of the ROS production was observed both in a short time treatment (Fig. 2A)

and a long time treatment (Fig. 2B). Under the same experimental conditions, Xn alone gives no

detectable fluorescence signal.

Physiological significance of targeting TrxR by 13n in HeLa cells. As we have

demonstrated the selective interaction of **13n** with TrxR in vitro and potent inhibition of TrxR in

HeLa cells, we then asked the physiological relevance of the cytotoxicity and TrxR inhibition by

13n. Pretreatment of HeLa cells with N-acetylcysteine (NAC), a thiol antioxidant and GSH

synthesis precursor in cells, confers cytoprotection against **13n**-induced cell death (Fig. 3A).

Subsequently, we determined the effect of GSH on the cytotoxicity of **13n**. Consistent with the

protection by NAC, inhibition of cellular GSH synthesis by BSO significantly enhances the

cytotoxicity of **13n** (Fig. 3B). Under our experimental conditions, pretreatment of HeLa cells with

50 μM BSO for 24 h decreases the cellular GSH level to ~30% of the control (Fig. S3 in SI). GSH

is a pivotal component of the glutathione network, which is another redox regulation system in

cells besides the thioredoxin system, and also acts as a backup of the thioredoxin system.[59]

Depletion of GSH sensitizing the cells to **13n** supports the involvement of the thioredoxin system

in the biological action of **13n**. To disclose the involvement of TrxR in the cytotoxicity of **13n**, we

turned to compare the sensitivity of HEK cells stably overexpressing TrxR1 (HEK-TrxR1) and

the cells that stably transfected with a vector (HEK-IRES) towards **13n** treatment. The TrxR1

expression level in HEK-TrxR1 cells are ~3--fold higher than that in HEK-IRES cells under our

experimental conditions.[43, 44] As shown in Fig. 4A, **13n** displays remarkably higher cytotoxicity to

HEK-IRES cells than HEK-TrxR1 cells. To further address the physiological significance of TrxR

in **13n**-induced cytotoxicity, we generated a cell line stably knocking down TrxR1 expression

(HeLa-shTrxR1 cells) by transfection of shRNA specifically targeting the enzyme. The TrxR1

expression level in HeLa-shTrxR1 cells is only about 20% of that in HeLa-shNT cells, which were

transfected with a non-targeting shRNA. Importantly, **13n** shows significantly elevating

cytotoxicity to HeLa-shTrxR1 cells (Fig. 4B). The efficiency of knockdown and overexpression

of TrxR1 in cells was fully evaluated in our recent publications.[43, 44] Collectively, our results

strongly supported that the biological action of **13n** in HeLa cells is dependent on its interaction

with TrxR.

Induction of apoptosis by 13n. It has been reported that Xn has ability to activate apoptotic

signaling in numerous type of malignant cells.[31, 32, 34, 38, 39, 60] Herein, we also demonstrated that

13n kills HeLa cells predominantly through the induction of apoptosis. When HeLa cells were

incubated with 2 μM or 5 μM of **13n** followed by Hoechst staining, an increasing number of cells

displayed condensed nuclei, a characteristic morphology of cells undergoing apoptosis (Fig. 5A).

Caspase 3 is a crucial component of the apoptotic machinery in different cell types, and the

activation of caspase 3 is a central event in the process of apoptosis. Thus, we next determined the

activity of caspase 3 after the cells exposure to **13n**. As shown in Fig. 5B, the caspase 3 activity in

HeLa cells was strikingly increased after treatment with varying concentrations of **13n**. Further

evidence from the annexin-V–fluorescein-5-isothiocyanate (FITC)/propidium iodide (PI) double

staining assay confirms that **13n** almost exclusively triggers apoptotic cell death in a

dose-dependent manner (Fig. 5C). Taken together, our data indicated that **13n** mainly induces

apoptotic cell death in HeLa cells.

TrxR is a pivotal component of the thioredoxin system, which is essential for maintaining the

cellular redox balance, and is involved in regulation of a wide range of redox signaling. The

malfunction of the system has been suggested to link to various diseases.[2] Inhibition of TrxR

reduces the available pool of reduced Trx, leading to a decrease in the activity of many enzyme

systems that require Trx as an electron donor,[1, 61] such as ribonucleotide reductase, peroxiredoxins,

and methionine sulfoxide reductases. Furthermore, the reduced Trx, but not the oxidized one,

directly interacts with a variety of apoptosis-related proteins, such as ASK1,[62] procaspase 3,[63]

AP-1[64] and NF-κB,[65] to suppress apoptosis, and thus TrxR inhibition promotes apoptosis.

Inhibition of TrxR is more detrimental to cancer cells as cancer cells generally require constant

DNA synthesis due to their fast proliferation, demand high antioxidant enzymes activity due to

their intrinsic elevated oxidative stress,[66] and display abrogation or resistance of apoptosis due to misregulated signaling pathways.[67] Targeting TrxR is a promising strategy to develop novel therapeutic agents.

Chalcones (1,3-diphenylpropen-1-ones) are naturally occurring compounds belonging to the flavonoid family and display a number of pharmacological functions.[26, 27] The presence of a double bond in conjugation with the carbonyl functionality (α, β-unsaturated ketone) is believed to be responsible for the biological activities of chalcones. Compounds with this structure in chemical libraries are usually considered as PAINS (Pan Assay Interference Compounds) which have the potential to cause misleading results in high-throughput screening.[68] The α, β-unsaturated ketone structure is one of the well-documented pharmacophores that targets the selenoprotein TrxR, which is the basis of the current work. All the synthesized compounds equally contain such structure, and the promising compound (**13n**) from the initial evaluation was fully determined to demonstrate its specific interaction with TrxR in the follow-up studies, thus precluding the false positive incidence. We have modified the substitute groups of Xn to furnish a series of Xn analogues. Based on the cytotoxicity screening results (Tables 1-3), preliminary structure-activity relationship could be drawn: 1) The prenyl group is not necessary for the activity, as **11m**, **11n**, **13h**, and **13n** are highly cytotoxic; 2) Molecules bearing electron-withdrawing groups (EWG), such as **8l**, **11m**, and **13l-p**, generally have better activity; 3) The EWG located at the *meta*-position (**11n** and **13n**) generally leads to higher activity than those at *orth*- or *para*-position (**11l** and **13l-p**); 4) Methylation of the hydroxyl groups on the benzene ring close to the carbonyl group commonly improves the potency, such as **11j** *vs* **13e**, **11k** *vs* **13o**, **11l** *vs* **13l**, **11m** *vs* **13m** and **11n** *vs* **13n**. The dispensability of the prenyl group for the activity would greatly

facilitate preparing more Xn analogues, as the introduction of the prenyl group is the most tedious step in synthesizing such kind of compounds (Step d in Scheme 1). We previously reported that several natural products bearing α, β-unsaturated ketone structure, such as curcumin,[45, 54] gambogic acid[43] and shikonin,[44] are potent TrxR inhibitors. In analogy to the inhibition of TrxR by those molecules, we reasoned that binding of **13n** to the enzyme might be the molecular basis for the inhibition of TrxR. The presence of the prenyl group makes the molecule steric and lipophilic, which is unfavorable for interacting with TrxR. Increasing the potency by removing the prenyl group would be another advantage for developing more potent TrxR inhibitors, as the steps of introducing the prenyl group are the most sluggish processes (Scheme 1, steps c and d) in synthesizing Xn analogues. Introducing the EWG to the molecules enhances the potency could be due to that the EWG makes the double bond more electron-deficient, thus facilitating the nucleophilic addition from TrxR. The potency of inhibition of TrxR by **13n** is moderate as several known TrxR inhibitors have lower IC_{50} values than **13n** does.[14, 15, 22, 43, 44] However, a great improvement has been achieved if comparing the potency of TrxR inhibition and cytotoxicity by **13n** to the lead natural product Xn. In this work, we kept the core chalcone structure, and mainly modified the benzene ring attached to the double bond. We are currently undergoing the structure modifications of the other benzene ring attached to the carbonyl group. We expected these further modifications would yield more potent TrxR inhibitors.

The specificity of **13n**-TrxR interaction was demonstrated by the following evidence. Firstly, we compared the in vitro inhibition of **13n** to TrxR, U498C TrxR, GR (a homologous to TrxR) and GPx (a Sec-containing enzyme) (Fig. 1). Single mutation of Sec to Cys sharply decreased the enzyme sensitivity to **13n**, indicating that the Sec residue in TrxR is a primary target for **13n**. The

structure of GR is quite closely related to TrxR, however, no apparent inhibition of GR was

observed under our experimental conditions. Furthermore, **13n** displays negligible effect to GPx,

which contains a buried Sec residue. The selective inhibition of WT TrxR, but not U498C TrxR,

GR or GPx, suggests a specific interaction of **13n** and TrxR. This selectivity could be due to the

binding of **13n** to the Sec residue as the Sec presents on the surface of the enzyme, and is more

reactive than Cys at physiological conditions. Secondly, we provided evidence in cellular context

to support the unique role of TrxR in **13n**'s biological action. HEK cells stably overexpressing

TrxR (HEK-TrxR1 cells) show less sensitivity to **13n** treatment compared to the cells only

transfected with the vector (HEK-IRES) (Fig. 4A). More physiologically relevant evidence that

genetic knockdown of TrxR elevates the compound's cytotoxicity further supports that TrxR is

critically involved in the biological function of **13n** (Fig. 4B). The glutathione system and

thioredoxin system are two major networks that work independently but with some overlaps in

regulating the intracellular redox balance. Recent studies suggested that the glutathione system

can act as a backup of the thioredoxin system.[59] Our observations that deletion of cellular GSH by

BSO enhances **13n**'s cytotoxicity, while elevation of GSH by NAC alleviates the cytotoxicity (Fig.

3), also support that TrxR is involved in the biological action of **13n**. Taken together, our data

suggest that **13n** targets TrxR in HeLa cells with high specificity.

Apoptosis is a consequence of a series of precisely controlled process that occurs in

physiological and pathological conditions, and is frequently altered in cancer cells. Two

well-known apoptosis signaling pathways, *i.e.*, the extrinsic cell surface receptor pathway and the

intrinsic mitochondrial pathway, converge on the caspases activation. Evading apoptosis, which

represents a major causative factor in the development and progression of cancer, is a hallmark in

diverse malignant cells arising from a complex interplay of genetic aberrations and misregulated

pathways.[67, 69] Our results indicated that compound **13n** shows potent cytotoxicity to HeLa cells

predominantly through induction of apoptosis (Fig. 5), thus potentiating the further development

of **13n** for treatment of tumors. ROS and mitochondria play an important role in apoptosis process.

Induction of ROS usually accompanies with the inhibition of TrxR.[15, 43-45] The elevated ROS level

impairs the mitochondria function, leading to release of cytochrome c to the cytocol, and

subsequently activates the caspases family. As we have observed that 13n could promote

accumulation of ROS (Fig. 2) and induction of apoptosis in HeLa cells (Fig. 5), it is most likely

that **13n** prompts apoptosis through the oxidative stress-induced intrinsic mitochondrial pathway.

CONCLUSIONS

In summary, we have synthesized Xn and its 43 analogues. After cytotoxicity screening, **13n** was

identified as the most cytotoxic compound towards HeLa cells with an IC_{50} value of 1.4 μM,

which is more than 30-fold increase of potency than the lead natural product Xn. Preliminary

structure-activity relationship study indicates that the prenyl group is not necessary for the

cytotoxicity, and introducing EWG, especially on the *meta*-position, into molecules is favored for

the activity. In addition, methylation of the hydroxyl groups on the benzene ring generally

improves the potency. The clarification of the structural determinants for the potency would guide

the design of novel potent molecules for future development. The follow-up studies discovered

that **13n** could selectively inhibit the redox enzyme TrxR in vitro, and effectively targets TrxR in

HeLa cells. Further mechanistic investigation revealed that **13n** could induce ROS production and

promote oxidative stress-mediated apoptosis in HeLa cells. The observation that cells

overexpressing TrxR are more resistant to **13n** insult, while knockdown of TrxR sensitizes cells to

13n treatment accentuates the physiological significance of targeting TrxR by **13n**.

EXPERIMENTAL PROCEDURES

Materials. The recombinant rat TrxR1 was essentially prepared as described[70], and is a gift

from Prof. Arne Holmgren at Karolinska Institute, Sweden. The recombinant U498C TrxR mutant

(Sec→Cys) and truncated TrxR (T-TrxR) were produced as described.[15, 71] The U498C TrxR is

active in DTNB assay, and the activity of the mutant enzyme is ~10% of that of the recombinant

wild type enzyme. Proteins were pure as judged by Coomassie-stained SDS-polyacrylamide gel

electrophoresis (PAGE). *E. coli* Trx was purchased from IMCO (Stockholm, Sweden,

www.imcocorp.se). RPMI 1640 Medium, Dulbecco's modified Eagle's medium (DMEM), G418,

NAC, bovine insulin, L-buthionine-(S,R)-sulfoximine (BSO),

N-acetyl-Asp-Glu-Val-Asp-p-nitroanilide (Ac-DEVD-pNA), reduced and oxidized glutathione

(GSH and GSSG), dimethyl sulfoxide (DMSO), yeast glutathione reductase (GR), glutathione

peroxidase (GPx), superoxide dismutase (SOD),

3-[(3-Cholamidopropyl)dimethylammonio]-1-propanesulfonate (CHAPS), DL-dithiothreitol

(DTT), puromycin and 2',7'-dichlorfluorescein diacetate (DCFH-DA) were obtained from

Sigma-Aldrich (St. Louis, USA). Cytochrome c and Ni-NTA-Sefinose were obtained from Sangon

Biotech (Shanghai, China). NADPH was obtained from Roche (Mannheim, Germany). Fetal

bovine serum (FBS) was obtained from Sijiqing (Hangzhou, China).

3-(4,5-Dimethylthiazol-2-yl)-2,5-diphenyltetrazolium bromide (MTT), penicillin and

streptomycin were obtained from Amresco (Solon, USA). Bovine serum albumin (BSA),

phenylmethylsulfonyl fluoride (PMSF), sodium orthovanadate (Na$_3$VO$_4$), ethylene diaminetetraacetic acid (EDTA) and 5,5'-dithiobis-2-nitrobenzoic acid (DTNB) were obtained from J&K Scientific (Beijing, China). Melting points (mp) were determined on a Fisher-Johns melting apparatus and were uncorrected.^{1}H NMR[13]C NMR spectra were recorded with a Bruker AMX spectrometer at 400 and 100 MHz, respectively, using TMS as the internal standard (chemical shifts are given in δ values, J is given in Hz). Mass spectra were obtained using a Hewlett-Packard 5988A spectrometer. The purity of final compounds was assessed by HPLC and was found to be higher than 95%. All other reagents were of analytical grade and were purchased from commercial supplies. All reactions were carried out under a deoxygenated and dry argon atmosphere unless otherwise indicated.

Compounds Purity Analysis. All final compounds were analyzed by HPLC to determine their purity. The analyses were performed on Waters 1525 2998 series HPLC system (C-18 column, Sun Fire, 5 μm, 4.6 mm×150 mm) at room temperature. Methanol and water were used as mobile phase, and the flow rate is 1.0 mL/min. The tested compounds were dissolved in methanol, and the injection volume is 10 μL. The maximal absorbance at the range of 210-400 nm was used as the detection wavelength.

Biological Studies

Cells and cell cultures. SMMC-7721, HeLa, HepG2, HL-60, and A549 cells were obtained from the Shanghai Institute of Biochemistry and Cell Biology, Chinese Academy of Sciences. HL-60 cells were cultured in RPMI 1640 supplemented with 10% FBS, 2 mM glutamine, and 100 units mL^{-1} penicillin/streptomycin and maintained in an atmosphere of 5% CO$_2$ at 37 °C. SMMC-7721 (7721), HeLa, A549 and HepG2 cells were cultured in DMEM with 10% FBS under

the same conditions. HEK-TrxR1 and HEK-IRES cells,[72] kindly provided by Prof. Constantinos Koumenis from University of Pennsylvania School of Medicine, were cultured in DMEM with 10% FBS, 2 mM glutamine, 100 units mL^{-1} penicillin/streptomycin, 0.1 μM sodium selenite, and 0.4 mg/mL G418 and maintained in an atmosphere of 5% CO_2 at 37 °C. The concentrations of DMSO in all cell experiments are 0.1% (V/V). The shRNA plasmid targeting coding regions of the TrxR1 gene (shTrxR1) and the control nontargeting shRNA (shNT)[73] were kindly provided by Prof. Constantinos Koumenis from University of Pennsylvania School of Medicine. HeLa cells were plated in a 6-well plate with 3×10^5 cells/well in DMEM media without antibiotics overnight and were transfected with either shTrxR1 (HeLa-shTrxR1) or shNT plasmid (HeLa-shNT) using Gene^{TM} III efficiency Transfection reagent (Biomiga, CA, USA). After 48 h of transfection, the cells were maintained with DMEM medium, 10% FBS, 2 mM glutamine, 100 units/mL penicillin/streptomycin at 37 °C in a humidified atmosphere of 5% CO_2, and selected by the supplement with 1 μg/mL puromycin for weeks.

Cytotoxicity Assays

MTT assay.[43, 44] Cells (5×10^3) were incubated with **13n** or its derivatives in triplicate in a 96-well plate for the indicated time at 37 °C in a final volume of 100 μL. Cells treated with DMSO alone were used as controls. At the end of the treatment (68 h), 10 μL MTT (5 mg/mL) was added to each well and incubated for an additional 4 h at 37 °C. An extraction buffer (100 μL, 10% SDS, 5% isobutanol, 0.1% HCl) was added, and the cells were incubated overnight at 37°C. The absorbance was measured at 570 nm on Multiskan GO (Thermo Scientific).

Trypan blue exclusion assay.[43, 44] HeLa cells were seeded in 24-well plates and treated with different concentrations of **13n** for 72 h. Cells treated with DMSO alone were used as controls,

16

and cell viability was determined by the trypan blue exclusion assay. After treatment, the cells were stained with trypan blue (0.4%, w/v), and the number of viable (non-stained) and dead (stained) cells were counted under a microscope.

Enzymes Activity Assays

GR assay.[43, 44] The NADPH-reduced GR (0.25 U/mL) in TE buffer (50 mM Tris-HCl with 1 mM EDTA, pH 7.5) was incubated with different concentrations of **13n** for 2 h in a 96-well plate at room temperature in a total volume of 100 µL. Reactions were initiated by the addition of the oxidized glutathione (GSSG) and NADPH (50 µL, final concentration: 1 mM and 400 µM, respectively). The GR activity was determined by measuring the decrease in absorbance at 340 nm during the initial 3 min. The same amounts of DMSO were added to the control experiments and the activity was expressed as the percentage of the control.

GPx assay.[15, 74] The GPx activity was measured indirectly by a coupled reaction with GR. GSSG, produced upon reduction of hydroperoxides by GPx, is recycled to its reduced state by GR and NADPH. The oxidation of NADPH to $NADP^+$ is accompanied by a decrease in absorbance at 340 nm. The rate of decrease in the A_{340} is directly proportional to the GPx activity. To the wells of a 96-well microliter plate were added 130 µL of TE buffer, 10 µL of a freshly prepared NADPH solution (4.0 mM in TE buffer), 10 µL of bovine erythrocyte GPx solution (1.0 $IU \cdot mL^{-1}$ in TE buffer), and 10 µL of indicated concentrations of 13n. The solution was incubated at 37 °C for 2 h. Then 10 µL of a baker's yeast GR solution (4.0 $IU \cdot mL^{-1}$ in TE buffer) and 10 µL of freshly prepared GSH solution (5.0 mM in TE buffer) were added. After adding 20 µL of H_2O_2 solution (5.0 mM in water), the final volume in each well was 200 µL. The background of GPx-independent NAPDH oxidation rate (r_1) was determined by replacing the GPx solution with

TE buffer. The rate of decrease in absorption of NADPH at 340 nm (r_2) was measured for 4 min at intervals of 10 sec at room temperature. The relative GPx activity was calculated by subtracting the r_1 from r_2, and was expressed as the percentage of the control.

In vitro TrxR activity by DTNB assay.[43, 44] The TrxR activity was determined at room temperature using a microplate reader. The NADPH-reduced TrxR (0.16 μM) or U498C TrxR (3.2 μM) was incubated with different concentrations of **13n** for 2 h at room temperature (the final volume of the mixture was 50 μL) in a 96-well plate. A master mixture in TE buffer (50 μL) containing DTNB and NADPH was added (final concentration: 2 mM and 200 μM, respectively), and the linear increase in absorbance at 412 nm during the initial 3 min was recorded. The same amounts of DMSO (0.1%, v/v) were added to the control experiments and the activity was expressed as the percentage of the control.

Determination of TrxR activity in HeLa cells.[43, 44] After HeLa cells were treated with different concentrations of **13n** for 48 h, the cells were harvested, and washed twice with PBS. Total cellular proteins were extracted by RIPA buffer (50 mM Tris-HCl pH 7.5, 2 mM EDTA, 0.5% deoxycholate, 150 mM NaCl, 1% Triton X-100, 0.1% SDS, 1 mM Na_3VO_4 and 1 mM PMSF) for 30 min on ice. The total protein content was quantified using the Bradford procedure. TrxR activity in cell lysates was measured by the endpoint insulin reduction assay. Briefly, the cell extract containing 20 μg of total proteins was incubated in a final reaction volume of 50 μl containing 100 mM Tris-HCl (pH 7.6), 0.3 mM insulin, 660 μM NADPH, 3 mM EDTA, and 15 μM *E. coli* Trx for 30 min at 37 °C. The reaction was terminated by adding 200 μL of 1 mM DTNB in 6 M guanidine hydrochloride, pH 8.0. A blank sample, containing everything except Trx, was treated in the same manner. The absorbance at 412 nm was measured, and the blank value

was subtracted from the corresponding absorbance value of the sample. The same amounts of DMSO were added to the control experiments and the activity was expressed as the percentage of the control.

Imaging TrxR activity in HeLa cells by TRFS-green.[15, 41] HeLa cells were treated with indicated concentrations of **13n** for 44 h, followed by treatment with TRFS-green (10 μM) for additional 4 h. The intensity of the green fluorescence in the cells correlates with the cellular TrxR activity. Phase contrast (top panel) and fluorescence (bottom panel) images were acquired with Floid[TM] cell imaging station (Life Technology).

Assessment of the intracellular ROS.[43, 44] HeLa cells were plated in 12-well plates and were treated with **13n** for 1 h. After removal of the medium, the ROS indicator DCFH-DA (10 μM) in fresh FBS-free medium was added, and continued incubation for 30 min at 37 °C in dark. The cells were visualized and photographed under a Leica inverted fluorescent microscopy.

Apoptosis Assays

Hoechst 33342 Staining.[43, 44] HeLa cells were plated in 12-well plates and were incubated with different concentrations of **13n** for 12 h followed by addition of Hoechst 33342 to a final concentration of 5 μg/mL. After incubation for additional 20 min, the cells were visualized and photographed under a Leica inverted fluorescent microscopy.

Measurement of caspase 3 activity.[43, 44] HeLa cells were treated with different concentrations of **13n** for 24 h in 100-mm dishes. The cells were collected, washed twice with PBS, and then lysed with RIPA buffer for 30 min on ice. The protein content was quantified using the Bradford procedure. A cell extract containing 50 μg of total proteins was incubated with the assay mixture (50 mM Hepes, 2 mM EDTA, 5% glycerol, 10 mM DTT, 0.1% CHAPS, 0.2 mM Ac-DEVD-pNA,

pH 7.5) for 3 h at 37 °C in a final volume of 100 μL. The absorbance at 405 nm was measured

using a microplate reader. The same amounts of DMSO were added to the control experiments

and the activity was expressed as the percentage of the control.

Annexin V/PI staining.[43, 44] HeLa cells were treated with varying concentrations of **13n** for

24 h in 60-mm dishes. The cells were harvested and washed with PBS. Apoptotic cells were

identified by double staining with FITC-conjugated Annexin V and PI according to the

manufacturer's instructions (Zoman Biotech, Beijing, China). The cells show four different cell

populations marked as follows: double-negative (unstained) cells showing live cell population,

FITC-positive and PI-negative stained cells showing early apoptosis, FITC/PI double-stained cells

showing late apoptosis, and finally PI-positive and FITC-negative stained cells showing necrotic

cells. Both the early apoptotic cells and the late apoptotic cells were designated as apoptotic cells.

Data were obtained and analyzed using Cellometer K2 Image Cytometer (Nexcelom Biosciences).

Statistics

Data are presented as mean ± S. E. Statistical differences between two groups were assessed

by the Students *t*-test. Comparisons among multiple groups were performed using one-way

analysis of variance (ANOVA), followed by a post hoc Scheffe test. $P<0.05$ was used as the

criterion for statistical significance.

ASSOCIATED CONTENT

Supporting Information

Inhibition of TrxR in vitro by different compounds, detection of cellular thiols after **13n** treatment,

determination of total glutathione after BSO treatment, and detailed synthetic procedures and

characterization of the compounds. This material is available free of charge via the Internet at

http://pubs.acs.org.

AUTHOR INFORMATION

Corresponding Author

*E-mail: fangjg@lzu.edu.cn; Tel: +86 931-8912500.

ACKNOWLEDGMENTS

ABBREVIATIONS USED

BSO: buthionine sulphoximine; DCFH: dichlorodihydrofluorescin; DCFH-DA: 2',

7'-dichlorofluorescin diacetate; DTT: DL-dithiothreitol; EWG: electron-withdrawing group; FITC:

fluorescein-5-isothiocyanate; GPx: glutathione peroxidase; GR: glutathione reductase; GSH:

reduced glutathione; GSSG: oxidized glutathione; HEK-IRES: HEK cells transfected with a

vector; HEK-TrxR1: HEK cells stably overexpressing TrxR1; HeLa-shNT: HeLa cells stably

transfected with a non-targeting shRNA; HeLa-shTrxR1: HeLa cells stably knocking down TrxR1;

MTT: 3-(4,5-dimethyl-2-thiazolyl)-2,5-diphenyl-2-H-tetrazolium bromide; NAC: N-acetylcysteine; PI: propidium iodide; ROS: reactive oxygen species; Sec: selenocysteine; TE buffer: 50 mM Tris-HCl with 1 mM EDTA, pH 7.5; Trx: thioredoxin; TrxR: thioredoxin reductase; Xn: xanthohumol.

REFERENCES

1. Lu, J.; Holmgren, A. The thioredoxin antioxidant system. *Free Radic. Biol. Med.* **2014,** *66*, 75-87.

2. Mahmood, D. F.; Abderrazak, A.; Khadija, E. H.; Simmet, T.; Rouis, M. The Thioredoxin System as a Therapeutic Target in Human Health and Disease. *Antioxid. Redox Signal.* **2013,** *19*, 1266-1303.

3. Bindoli, A.; Rigobello, M. P. Principles in redox signaling: from chemistry to functional significance. *Antioxid. Redox Signal.* **2013,** *18*, 1557-1593.

4. Zhong, L.; Arner, E. S.; Holmgren, A. Structure and mechanism of mammalian thioredoxin reductase: the active site is a redox-active selenolthiol/selenenylsulfide formed from the conserved cysteine-selenocysteine sequence. *Proc. Natl. Acad. Sci. U. S. A.* **2000,** *97*, 5854-5859.

5. Gladyshev, V. N.; Jeang, K. T.; Stadtman, T. C. Selenocysteine, identified as the penultimate C-terminal residue in human T-cell thioredoxin reductase, corresponds to TGA in the human placental gene. *Proc. Natl. Acad. Sci. U. S. A.* **1996,** *93*, 6146-6151.

6. Cai, W.; Zhang, L.; Song, Y.; Wang, B.; Zhang, B.; Cui, X.; Hu, G.; Liu, Y.; Wu, J.; Fang, J. Small molecule inhibitors of mammalian thioredoxin reductase. *Free Radic. Biol. Med.* **2012,** *52*,

257-265.

7. Arner, E. S. Focus on mammalian thioredoxin reductases--important selenoproteins with versatile functions. *Biochim. Biophys. Acta.* **2009,** *1790*, 495-526.

8. Kahlos, K.; Soini, Y.; Saily, M.; Koistinen, P.; Kakko, S.; Paakko, P.; Holmgren, A.; Kinnula, V. L. Up-regulation of thioredoxin and thioredoxin reductase in human malignant pleural mesothelioma. *Int. J. Cancer* **2001,** *95*, 198-204.

9. Berggren, M.; Gallegos, A.; Gasdaska, J. R.; Gasdaska, P. Y.; Warneke, J.; Powis, G. Thioredoxin and thioredoxin reductase gene expression in human tumors and cell lines, and the effects of serum stimulation and hypoxia. *Anticancer Res.* **1996,** *16*, 3459-3466.

10. Kim, S. J.; Miyoshi, Y.; Taguchi, T.; Tamaki, Y.; Nakamura, H.; Yodoi, J.; Kato, K.; Noguchi, S. High thioredoxin expression is associated with resistance to docetaxel in primary breast cancer. *Clin. Cancer Res.* **2005,** *11*, 8425-8430.

11. Yoo, M. H.; Xu, X. M.; Carlson, B. A.; Patterson, A. D.; Gladyshev, V. N.; Hatfield, D. L. Targeting thioredoxin reductase 1 reduction in cancer cells inhibits self-sufficient growth and DNA replication. *PLoS One* **2007,** *2*, e1112.

12. Yoo, M. H.; Xu, X. M.; Carlson, B. A.; Gladyshev, V. N.; Hatfield, D. L. Thioredoxin reductase 1 deficiency reverses tumor phenotype and tumorigenicity of lung carcinoma cells. *J. Biol. Chem.* **2006,** *281*, 13005-13008.

13. Zou, T.; Lum, C. T.; Lok, C. N.; To, W. P.; Low, K. H.; Che, C. M. A binuclear gold(I) complex with mixed bridging diphosphine and bis(N-heterocyclic carbene) ligands shows favorable thiol reactivity and inhibits tumor growth and angiogenesis in vivo. *Angew. Chem. Int. Ed. Engl.* **2014,** *53*, 5810-5814.

14. Zhang, D.; Xu, Z.; Yuan, J.; Zhao, Y. X.; Qiao, Z. Y.; Gao, Y. J.; Yu, G. A.; Li, J.; Wang, H. Synthesis and molecular recognition studies on small-molecule inhibitors for thioredoxin reductase. *J. Med. Chem.* **2014,** *57*, 8132-8139.

15. Liu, Y.; Duan, D.; Yao, J.; Zhang, B.; Peng, S.; Ma, H.; Song, Y.; Fang, J. Dithiaarsanes induce oxidative stress-mediated apoptosis in HL-60 cells by selectively targeting thioredoxin reductase. *J. Med. Chem.* **2014,** *57*, 5203-5211.

16. Huang, L.; Chen, Y.; Liang, B.; Xing, B.; Wen, G.; Wang, S.; Yue, X.; Zhu, C.; Du, J.; Bu, X. A furanyl acryl conjugated coumarin as an efficient inhibitor and a highly selective off-on fluorescent probe for covalent labelling of thioredoxin reductase. *Chem. Commun.* **2014,** *50*, 6987-6990.

17. Sun, R. W. Y.; Lok, C. N.; Fong, T. T. H.; Li, C. K. L.; Yang, Z. F.; Zou, T.; Siu, A. F. M.; Che, C. M. A dinuclear cyclometalated gold(III)–phosphine complex targeting thioredoxin reductase inhibits hepatocellular carcinoma in vivo. *Chem. Sci.* **2013,** *4*, 1979-1988.

18. Oehninger, L.; Kuster, L. N.; Schmidt, C.; Munoz-Castro, A.; Prokop, A.; Ott, I. A chemical-biological evaluation of rhodium(I) N-heterocyclic carbene complexes as prospective anticancer drugs. *Chem. Eur. J.* **2013,** *19*, 17871-17880.

19. Schuh, E.; Pfluger, C.; Citta, A.; Folda, A.; Rigobello, M. P.; Bindoli, A.; Casini, A.; Mohr, F. Gold(I) carbene complexes causing thioredoxin 1 and thioredoxin 2 oxidation as potential anticancer agents. *J. Med. Chem.* **2012,** *55*, 5518-5528.

20. Meyer, A.; Bagowski, C. P.; Kokoschka, M.; Stefanopoulou, M.; Alborzinia, H.; Can, S.; Vlecken, D. H.; Sheldrick, W. S.; Wolfl, S.; Ott, I. On the biological properties of alkynyl phosphine gold(I) complexes. *Angew. Chem. Int. Ed. Engl.* **2012,** *51*, 8895-8899.

21. Citta, A.; Schuh, E.; Mohr, F.; Folda, A.; Massimino, M. L.; Bindoli, A.; Casini, A.; Rigobello, M. P. Fluorescent silver(I) and gold(I)-N-heterocyclic carbene complexes with cytotoxic properties: mechanistic insights. *Metallomics* **2013,** *5*, 1006-1015.

22. Citta, A.; Folda, A.; Bindoli, A.; Pigeon, P.; Top, S.; Vessieres, A.; Salmain, M.; Jaouen, G.; Rigobello, M. P. Evidence for targeting thioredoxin reductases with ferrocenyl quinone methides. A possible molecular basis for the antiproliferative effect of hydroxyferrocifens on cancer cells. *J. Med. Chem.* **2014,** *57*, 8849-8859.

23. Kingston, D. G. Modern natural products drug discovery and its relevance to biodiversity conservation. *J. Nat. Prod.* **2011,** *74*, 496-511.

24. Koehn, F. E.; Carter, G. T. The evolving role of natural products in drug discovery. *Nat. Rev. Drug Discov.* **2005,** *4*, 206-220.

25. Newman, D. J. Natural products as leads to potential drugs: an old process or the new hope for drug discovery? *J. Med. Chem.* **2008,** *51*, 2589-2599.

26. Singh, P.; Anand, A.; Kumar, V. Recent developments in biological activities of chalcones: A mini review. *Eur. J. Med. Chem.* **2014,** *85C*, 758-777.

27. Sahu, N. K.; Balbhadra, S. S.; Choudhary, J.; Kohli, D. V. Exploring pharmacological significance of chalcone scaffold: a review. *Curr. Med. Chem.* **2012,** *19*, 209-225.

28. Jain, M. G.; Hislop, G. T.; Howe, G. R.; Burch, J. D.; Ghadirian, P. Alcohol and other beverage use and prostate cancer risk among Canadian men. *Int. J. Cancer* **1998,** *78*, 707-711.

29. Gerhauser, C. Beer constituents as potential cancer chemopreventive agents. *Eur. J. Cancer* **2005,** *41*, 1941-1954.

30. Blanquer-Rossello, M. M.; Oliver, J.; Valle, A.; Roca, P. Effect of xanthohumol and

8-prenylnaringenin on MCF-7 breast cancer cells oxidative stress and mitochondrial complexes expression. *J. Cell. Biochem.* **2013,** *114*, 2785-2794.

31. Festa, M.; Capasso, A.; D'Acunto, C. W.; Masullo, M.; Rossi, A. G.; Pizza, C.; Piacente, S. Xanthohumol induces apoptosis in human malignant glioblastoma cells by increasing reactive oxygen species and activating MAPK pathways. *J. Nat. Prod.* **2011,** *74*, 2505-2513.

32. Strathmann, J.; Klimo, K.; Sauer, S. W.; Okun, J. G.; Prehn, J. H.; Gerhauser, C. Xanthohumol-induced transient superoxide anion radical formation triggers cancer cells into apoptosis via a mitochondria-mediated mechanism. *FASEB J.* **2010,** *24*, 2938-2950.

33. Kang, Y.; Park, M. A.; Heo, S. W.; Park, S. Y.; Kang, K. W.; Park, P. H.; Kim, J. A. The radio-sensitizing effect of xanthohumol is mediated by STAT3 and EGFR suppression in doxorubicin-resistant MCF-7 human breast cancer cells. *Biochim. Biophys. Acta* **2013,** *1830*, 2638-2648.

34. Deeb, D.; Gao, X.; Jiang, H.; Arbab, A. S.; Dulchavsky, S. A.; Gautam, S. C. Growth inhibitory and apoptosis-inducing effects of xanthohumol, a prenylated chalone present in hops, in human prostate cancer cells. *Anticancer Res.* **2010,** *30*, 3333-3339.

35. Harikumar, K. B.; Kunnumakkara, A. B.; Ahn, K. S.; Anand, P.; Krishnan, S.; Guha, S.; Aggarwal, B. B. Modification of the cysteine residues in IkappaBalpha kinase and NF-kappaB (p65) by xanthohumol leads to suppression of NF-kappaB-regulated gene products and potentiation of apoptosis in leukemia cells. *Blood* **2009,** *113*, 2003-2013.

36. Albini, A.; Dell'Eva, R.; Vene, R.; Ferrari, N.; Buhler, D. R.; Noonan, D. M.; Fassina, G. Mechanisms of the antiangiogenic activity by the hop flavonoid xanthohumol: NF-kappaB and Akt as targets. *FASEB J.* **2006,** *20*, 527-529.

37. Monteghirfo, S.; Tosetti, F.; Ambrosini, C.; Stigliani, S.; Pozzi, S.; Frassoni, F.; Fassina, G.; Soverini, S.; Albini, A.; Ferrari, N. Antileukemia effects of xanthohumol in Bcr/Abl-transformed cells involve nuclear factor-kappaB and p53 modulation. *Mol. Cancer Ther.* **2008,** *7*, 2692-2702.

38. Pan, L.; Becker, H.; Gerhauser, C. Xanthohumol induces apoptosis in cultured 40-16 human colon cancer cells by activation of the death receptor- and mitochondrial pathway. *Mol. Nutr. Food Res.* **2005,** *49*, 837-843.

39. Gerhauser, C.; Alt, A.; Heiss, E.; Gamal-Eldeen, A.; Klimo, K.; Knauft, J.; Neumann, I.; Scherf, H. R.; Frank, N.; Bartsch, H.; Becker, H. Cancer chemopreventive activity of Xanthohumol, a natural product derived from hop. *Mol. Cancer Ther.* **2002,** *1*, 959-969.

40. Miranda, C. L.; Aponso, G. L.; Stevens, J. F.; Deinzer, M. L.; Buhler, D. R. Prenylated chalcones and flavanones as inducers of quinone reductase in mouse Hepa 1c1c7 cells. *Cancer Lett.* **2000,** *149*, 21-29.

41. Zhang, L.; Duan, D.; Liu, Y.; Ge, C.; Cui, X.; Sun, J.; Fang, J. Highly Selective Off-On Fluorescent Probe for Imaging Thioredoxin Reductase in Living Cells. *J. Am. Chem. Soc.* **2014,** *136*, 226-233.

42. Yao, J.; Ge, C.; Duan, D.; Zhang, B.; Cui, X.; Peng, S.; Liu, Y.; Fang, J. Activation of the Phase II Enzymes for Neuroprotection by Ginger Active Constituent 6-Dehydrogingerdione in PC12 Cells. *J. Agric. Food Chem.* **2014,** *62*, 5507-5518.

43. Duan, D.; Zhang, B.; Yao, J.; Liu, Y.; Sun, J.; Ge, C.; Peng, S.; Fang, J. Gambogic acid induces apoptosis in hepatocellular carcinoma SMMC-7721 cells by targeting cytosolic thioredoxin reductase. *Free Radic. Biol. Med.* **2014,** *69*, 15-25.

44. Duan, D.; Zhang, B.; Yao, J.; Liu, Y.; Fang, J. Shikonin targets cytosolic thioredoxin

reductase to induce ROS-mediated apoptosis in human promyelocytic leukemia HL-60 cells. *Free Radic. Biol. Med.* **2014,** *70*, 182-193.

45. Cai, W.; Zhang, B.; Duan, D.; Wu, J.; Fang, J. Curcumin targeting the thioredoxin system elevates oxidative stress in HeLa cells. *Toxicol Appl Pharmacol* **2012,** 262, 341-348.

46. Zhang, L. W.; Duan, D. Z.; Cui, X. M.; Sun, J. Y.; Fang, J. G. A selective and sensitive fluorescence probe for imaging endogenous zinc in living cells. *Tetrahedron* **2013,** *69*, 15-21.

47. Zhang, B.; Ge, C.; Yao, J.; Liu, Y.; Xie, H.; Fang, J. Selective selenol fluorescent probes: design, synthesis, structural   determinants, and biological applications. *J. Am. Chem. Soc.* **2015**, *137*, 757-769.

48. Kumar, V.; Kumar, S.; Hassan, M.; Wu, H.; Thimmulappa, R. K.; Kumar, A.; Sharma, S. K.; Parmar, V. S.; Biswal, S.; Malhotra, S. V. Novel chalcone derivatives as potent Nrf2 activators in mice and human lung epithelial cells. *J. Med. Chem.* **2011,** *54*, 4147-4159.

49. Zhu, C.; Zuo, Y.; Wang, R.; Liang, B.; Yue, X.; Wen, G.; Shang, N.; Huang, L.; Chen, Y.; Du, J.; Bu, X. Discovery of potent cytotoxic ortho-aryl chalcones as new scaffold targeting tubulin and mitosis with affinity-based fluorescence. *J. Med. Chem.* **2014,** *57*, 6364-6382.

50. Khupse, R. S.; Erhardt, P. W. Total synthesis of xanthohumol. *J. Nat. Prod.* **2007,** *70*, 1507-1509.

51. Gan, F. F.; Kaminska, K. K.; Yang, H.; Liew, C. Y.; Leow, P. C.; So, C. L.; Tu, L. N.; Roy, A.; Yap, C. W.; Kang, T. S.; Chui, W. K.; Chew, E. H. Identification of Michael acceptor-centric pharmacophores with substituents that yield strong thioredoxin reductase inhibitory character correlated to antiproliferative activity. *Antioxid. Redox Signal.* **2013,** *19*, 1149-1165.

52. Chew, E. H.; Nagle, A. A.; Zhang, Y.; Scarmagnani, S.; Palaniappan, P.; Bradshaw, T. D.;

Holmgren, A.; Westwell, A. D. Cinnamaldehydes inhibit thioredoxin reductase and induce Nrf2: potential candidates for cancer therapy and chemoprevention. *Free Radic. Biol. Med.* **2010,** *48,* 98-111.

53. Fang, J.; Holmgren, A. Inhibition of thioredoxin and thioredoxin reductase by 4-hydroxy-2-nonenal in vitro and in vivo. *J. Am. Chem. Soc.* **2006,** *128,* 1879-1885.

54. Fang, J.; Lu, J.; Holmgren, A. Thioredoxin reductase is irreversibly modified by curcumin: a novel molecular mechanism for its anticancer activity. *J. Biol. Chem.* **2005,** *280,* 25284-25290.

55. Holmgren, A.; Bjornstedt, M. Thioredoxin and thioredoxin reductase. *Methods Enzymol.* **1995,** *252,* 199-208.

56. Laurent, T. C.; Moore, E. C.; Reichard, P. Enzymatic Synthesis of Deoxyribonucleotides. Iv. Isolation and Characterization of Thioredoxin, the Hydrogen Donor from Escherichia Coli B. *J. Biol. Chem.* **1964,** *239,* 3436-3444.

57. Chae, H. Z.; Chung, S. J.; Rhee, S. G. Thioredoxin-dependent peroxide reductase from yeast. *J. Biol. Chem.* **1994,** *269,* 27670-27678.

58. Gonzalez Porque, P.; Baldesten, A.; Reichard, P. The involvement of the thioredoxin system in the reduction of methionine sulfoxide and sulfate. *J. Biol. Chem.* **1970,** *245,* 2371-2374.

59. Du, Y.; Zhang, H.; Lu, J.; Holmgren, A. Glutathione and glutaredoxin act as a backup of human thioredoxin reductase 1 to reduce thioredoxin 1 preventing cell death by aurothioglucose. *J. Biol. Chem.* **2012,** *287,* 38210-38219.

60. Colgate, E. C.; Miranda, C. L.; Stevens, J. F.; Bray, T. M.; Ho, E. Xanthohumol, a prenylflavonoid derived from hops induces apoptosis and inhibits NF-kappaB activation in prostate epithelial cells. *Cancer Lett.* **2007,** *246,* 201-209.

61. Nordberg, J.; Arner, E. S. Reactive oxygen species, antioxidants, and the mammalian thioredoxin system. *Free Radic. Biol. Med.* **2001,** *31*, 1287-1312.

62. Saitoh, M.; Nishitoh, H.; Fujii, M.; Takeda, K.; Tobiume, K.; Sawada, Y.; Kawabata, M.; Miyazono, K.; Ichijo, H. Mammalian thioredoxin is a direct inhibitor of apoptosis signal-regulating kinase (ASK) 1. *EMBO J.* **1998,** *17*, 2596-2606.

63. Mitchell, D. A.; Morton, S. U.; Fernhoff, N. B.; Marletta, M. A. Thioredoxin is required for S-nitrosation of procaspase-3 and the inhibition of apoptosis in Jurkat cells. *Proc. Natl. Acad. Sci. U. S. A.* **2007,** *104*, 11609-11614.

64. Hirota, K.; Matsui, M.; Iwata, S.; Nishiyama, A.; Mori, K.; Yodoi, J. AP-1 transcriptional activity is regulated by a direct association between thioredoxin and Ref-1. *Proc. Natl. Acad. Sci. U. S. A.* **1997,** *94*, 3633-3638.

65. Matthews, J. R.; Wakasugi, N.; Virelizier, J. L.; Yodoi, J.; Hay, R. T. Thioredoxin regulates the DNA binding activity of NF-kappa B by reduction of a disulphide bond involving cysteine 62. *Nucleic Acids Res.* **1992,** *20*, 3821-3830.

66. Trachootham, D.; Alexandre, J.; Huang, P. Targeting cancer cells by ROS-mediated mechanisms: a radical therapeutic approach? *Nat. Rev. Drug Discov.* **2009,** *8*, 579-591.

67. Hanahan, D.; Weinberg, R. A. Hallmarks of cancer: the next generation. *Cell* **2011,** *144*, 646-674.

68. Baell, J. B.; Holloway, G. A. New substructure filters for removal of pan assay interference compounds (PAINS) from screening libraries and for their exclusion in bioassays. *J. Med. Chem.* **2010,** *53*, 2719-2740.

69. Fernald, K.; Kurokawa, M. Evading apoptosis in cancer. *Trends Cell Biol.* **2013,** *23*, 620-633.

70. Arner, E. S.; Sarioglu, H.; Lottspeich, F.; Holmgren, A.; Bock, A. High-level expression in

Escherichia coli of selenocysteine-containing rat thioredoxin reductase utilizing gene fusions with

engineered bacterial-type SECIS elements and co-expression with the selA, selB and selC genes.

J. Mol. Biol. **1999,** *292*, 1003-1016.

71. Zhong, L. W.; Holmgren, A. Essential role of selenium in the catalytic activities of

mammalian thioredoxin reductase revealed by characterization of recombinant enzymes with

selenocysteine mutations. *J. Biol. Chem.* **2000,** *275*, 18121-18128.

72. Nalvarte, I.; Damdimopoulos, A. E.; Nystom, C.; Nordman, T.; Miranda-Vizuete, A.; Olsson,

J. M.; Eriksson, L.; Bjornstedt, M.; Arner, E. S.; Spyrou, G. Overexpression of enzymatically

active human cytosolic and mitochondrial thioredoxin reductase in HEK-293 cells. Effect on cell

growth and differentiation. *J. Biol. Chem.* **2004,** *279*, 54510-54517.

73. Javvadi, P.; Hertan, L.; Kosoff, R.; Datta, T.; Kolev, J.; Mick, R.; Tuttle, S. W.; Koumenis, C.

Thioredoxin reductase-1 mediates curcumin-induced radiosensitization of squamous carcinoma

cells. *Cancer Res.* **2010,** *70*, 1941-1950.

74. Mills, G. C. The purification and properties of glutathione peroxidase of erythrocytes. *J. Biol.

Chem.* **1959,** *234*, 502-506.

31

Table 1. Cytotoxicity screening of compounds **8a-8m**.

Compd.	R₁	R₂	R₃	R₄	R₅	IC$_{50}$ /(μM)*		
						A549	HeLa	Hep G2
8a (Xn)	H	H	OH	H	H	30.5±2.3	40.4±2.1	35.0±1.8
8b	H	H	OMe	H	H	38.0±1.5	>50	32.4±2.2
8c	H	OMe	OH	H	H	11.8±1.1	33.8±1.8	21.7±0.9
8d	H	OH	OH	H	H	16.1±1.2	38.1±1.6	15.2±0.2
8e	OMe	H	H	H	H	12.5±2.2	19.7±1.1	14.6±0.8
8f	H	OMe	OMe	H	H	15.7±0.9	27.7±1.3	13.8±1.8
8g	OMe	OMe	OMe	H	H	18±2.1	>50	14.8±2.1
8h	OMe	H	OMe	OMe	H	14.4±1.5	>50	>50
8i	H	OMe	OMe	OMe	H	>50	>50	>50
8j	H	H	Cl	H	H	11.8±1.5	16.5±1.1	10.1±1.9
8k	H	H	NO₂	H	H	31.2±1.4	29.7±1.7	12.4±2.1
8l	H	H	CF₃	H	H	11.1±1.2	6.8±1.0	6.5±0.8
8m	H	NO₂	H	H	H	15.0±2.1	16.5±2.0	16.6±0.6

* The cell viability was determined by the MTT assay after a 72-h treatment.

Table 2. Cytotoxicity screening of compounds **11a-11n**.

Compd.	R_1	R_2	R_3	R_4	R_5	IC_{50} /(μM)*		
						A549	HeLa	Hep G2
11a	H	H	OH	H	H	>50	48.1±1.4	40.2±0.9
11b	H	H	OMe	H	H	>50	47.7±2.0	18.1±1.1
11c	OMe	H	H	H	H	47.7±1.2	43.6±1.9	15.3±0.8
11d	H	H	Me	H	H	>50	>50	>50
11e	H	OMe	OH	H	H	>50	>50	>50
11f	H	OMe	OMe	H	H	>50	49.5±1.1	18.5±1.7
11g	H	OMe	H	OMe	H	34.0±1.5	13.3±2.1	17.6±1.4
11h	OMe	H	OMe	OMe	H	34.2±0.5	37.8±1.4	18.7±1.6
11i	H	OMe	OMe	OMe	H	28.4±2.1	18.9±2.4	20.4±0.5
11j	H	OH	OH	H	H	11.8±1.4	21.3±0.9	28.7±1.3
11k	H	H	Cl	H	H	18.2±2.1	17.0±1.6	12.2±1.1
11l	H	H	NO$_2$	H	H	>50	>50	41.0±1.5
11m	H	H	CF$_3$	H	H	15.4±1.5	9.5±2.2	14.1±1.3
11n	H	NO$_2$	H	H	H	36.8±1.5	15.5±0.9	16.3±0.4

* The cell viability was determined by the MTT assay after a 72-h treatment.

33

Table 3. Cytotoxicity screening of compounds **13a-13q**.

| Compd.	R$_1$	R$_2$	R$_3$	R$_4$	R$_5$	IC$_{50}$ /(μM)*		
						A549	HeLa	Hep G2
13a	H	H	OH	H	H	49.4±0.3	40.6±1.2	37.0±1.1
13b	H	H	OMe	H	H	46.6±2.1	19.6±1.6	13.5±1.9
13c	OMe	H	H	H	H	19.8±0.9	19.6±1.2	16.3±1.1
13d	H	H	Me	H	H	15.0±2.1	17.0±1.4	18.4±1.9
13e	H	OH	OH	H	H	8.2±1.5	15.8±2.1	27.5±1.3
13f	H	OMe	OH	H	H	43.8±1.1	44.9±1.3	17.0±2.0
13g	H	OMe	OMe	H	H	39.1±0.8	18.1±1.2	11.6±1.0
13h	H	OMe	H	OMe	H	10.1±0.9	9.2±1.2	9.0±1.8
13i	H	OMe	OMe	OMe	H	22.3±1.9	9.9±0.8	16.5±1.4
13j	OMe	H	OMe	OMe	H	45.1±2.1	40.5±1.3	23.8±1.5
13k	OMe	OMe	OMe	H	H	44.3±	>50	>50
13l	H	H	NO$_2$	H	H	7.1±1.1	8.0±1.4	9.4±0.9
13m	H	H	CF$_3$	H	H	14.2±1.1	5.1±0.5	9.7±1.2
13n	H	NO$_2$	H	H	H	5.4±1.1	1.4±0.2	4.9±0.7
13o	H	H	Cl	H	H	13.3±1.6	3.9±0.8	12.4±1.1
13p	NO$_2$	H	H	H	H	10.7±0.9	9.0±1.2	7.9±1.5
13q	H	H	NH$_2$	H	H	>50	>50	45.2±2.3

* The cell viability was determined by the MTT assay after a 72-h treatment.

Table 4. Cytotoxicity of **8l**, **11n**, **13m**, **13n** and **13o**.

Compd.	IC_{50} (μM)*			
	HeLa	A549	7721	HL-60
8l	6.8 ± 1.0	11.1 ± 1.2	10.7 ± 1.4	5.3 ± 1.5
11n	15.5 ± 0.9	36.8 ± 1.5	20.1 ± 1.0	5.9 ± 0.8
13m	5.1 ± 0.5	14.2 ± 1.1	15.7 ± 0.1	6.5 ± 1.0
13n	1.4 ± 0.2	5.4 ± 1.1	4.2 ± 0.6	1.6 ± 0.5
	1.7 ± 0.1**			
13o	3.9 ± 0.8	13.3 ± 1.6	11.7 ± 0.8	4.2 ± 1.2

* The data were obtained by the MTT assay after a 72-h treatment.

** This value was from the trypan blue exclusion assay.

**Scheme 1.** Synthesis of compounds **8a-8m.**
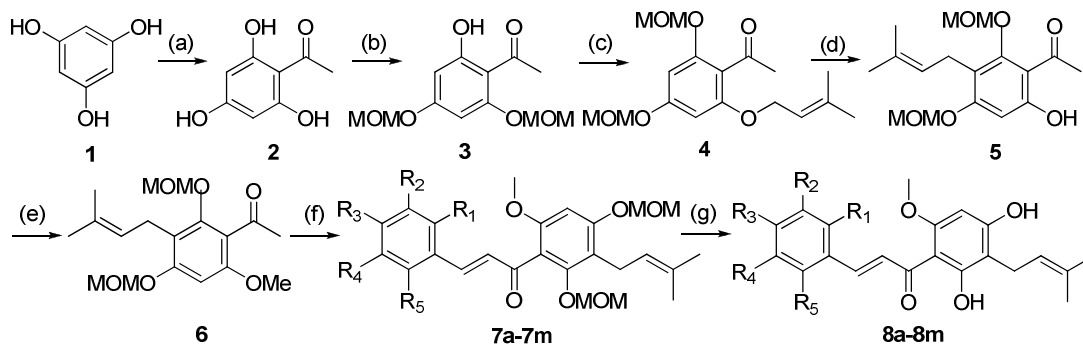
Reagents and conditions : (a) BF$_3$.Et$_2$O, Ac$_2$O, 90-100 °C; (b) DIPEA, MOMOCl, DCM, rt; (c) Prenyl bromide, K$_2$CO$_3$, acetone, reflux; (d) N,N-Dimethylaniline, 200-220 °C; (e) MeI, DMF, K$_2$CO$_3$, rt; (f) Anhydrous methanol, KOH, aldehyde, rt; (g) Anhydrous methanol, HCl, reflux.

Scheme 2. Synthesis of compounds **11a-11n.**
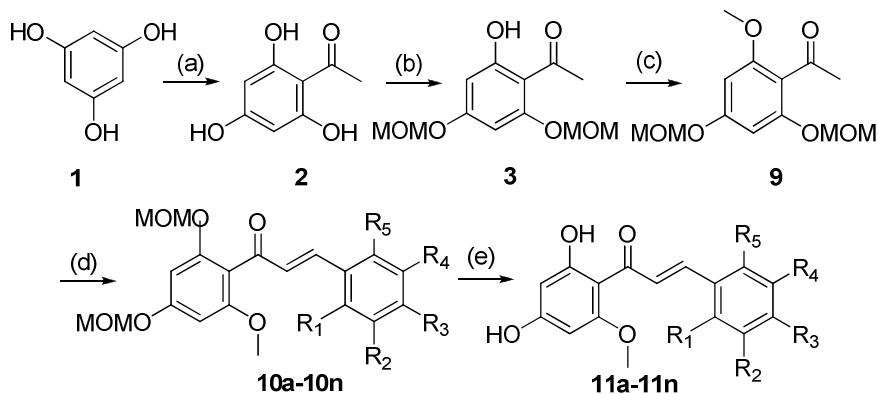
Reagents and conditions : (a) BF$_3$.Et$_2$O, Ac$_2$O, 90-100 °C; (b) DIPEA, MOMOCl, DCM, rt; (c) MeI, DMF, K$_2$CO$_3$, rt; (d) Anhydrous methanol, KOH, aldehyde, rt; (e) Anhydrous methanol, HCl, reflux.

**Scheme 3.** Synthesis of compounds **13a-13q.**
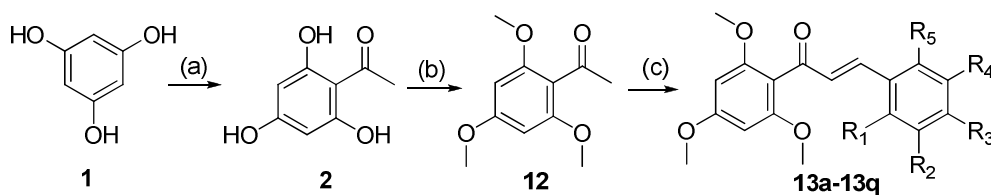
Reagents and conditions : (a) BF$_3$.Et$_2$O, Ac$_2$O, 90-100 °C; (b) MeI, DMF, K$_2$CO$_3$, rt; (c) Anhydrous methanol, KOH, aldehyde, rt.
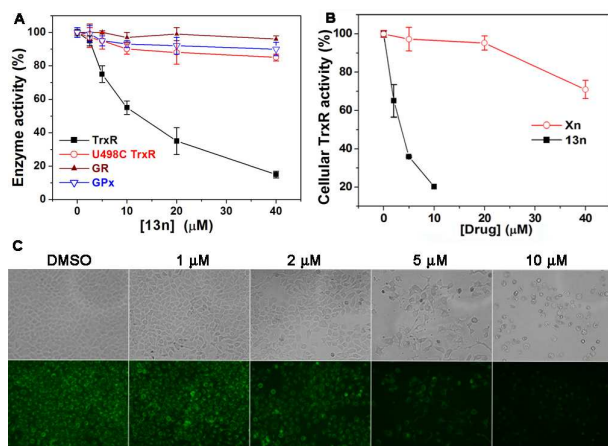
Figure 1. Inhibition of TrxR by **13n**. (A) Inhibition of TrxR, U498C TrxR , GPx and GR by 13n. The enzymes were incubated with the indicated concentrations of **13n** for 2h at room temperature, and the enzyme's activity was determined as described in Materials and Methods. All the activity was expressed as the percentage of the control. (B) Inhibition of TrxR by 13n and Xn in HeLa cells. The HeLa cells were treated with the indicated concentrations of **13n** for 48 h, the enzyme activity of TrxR in the cells was determined by the endpoint insulin reduction assay. (C) Imaging TrxR activity in live HeLa cells. The HeLa cells were treated with the indicated concentrations of **13n** for 44 h, followed by further treatment with TRFS-green for 4 h. The fluorescence images were acquired by inverted fluorescence microscopy. Data are expressed as mean ± S. E. of three experiments.
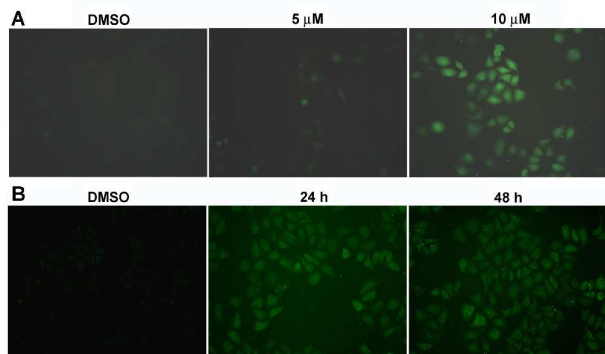
Figure 2. Induction of ROS in HeLa cells. (A) The HeLa Cells were treated with different concentrations of **13n** for 1 h followed by the incubation with the fluorescence probe DCFH-DA (10 μM) for 30 min. (B) The HeLa Cells were treated with a fixed concentration of **13n** (2 μM) for 24 h and 48 h followed by the incubation with the fluorescence probe DCFH-DA (10 μM) for 30 min. The fluorescence images were acquired by inverted fluorescence microscopy.
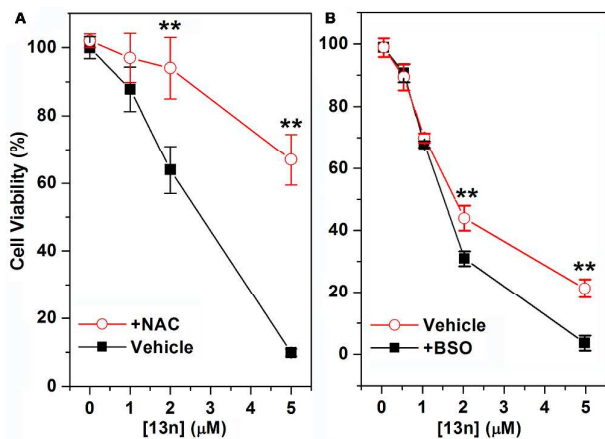
Figure 3. Effects of NAC and GSH on the cytotoxicity of **13n**. (A) Protection of the cells by NAC.

HeLa cells were incubated with the indicated concentrations of **13n** and NAC (1 mM) for 48 h.

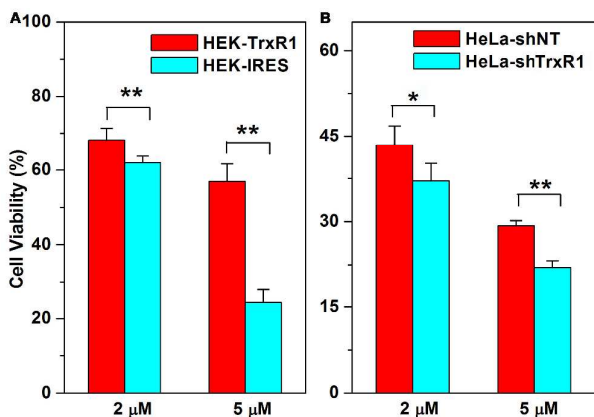The cell viability was determined by the MTT assay. Data are expressed as mean ± S. E. of three

experiments. (B) Augmentation of the cytotoxicity by GSH depletion. The HeLa cells were

treated with 50 μM BSO for 24 h to lower the intracellular GSH level, followed by 13n treatment

for an additional 48 h. The cell viability was determined by the MTT assay. Data are expressed as

mean ± S. E. of three experiments. *, $P < 0.05$, **, $P < 0.01$, vs. the control group.

Figure 4. Involvement of TrxR in the cytotoxicity of **13n**. (A) Cytotoxic effects of 13n on HEK-IRES and HEK-TrxR1 cells. The cells were treated with the indicated concentrations of **13n** for 72 h, and the cell viability was determined by the MTT assay. Data are expressed as mean ±S. E. of three experiments (B) Cytotoxic effects of 13n on HeLa-shNT and HeLa-shTrxR1 cells. The cells were treated with the indicated concentrations of **13n** for 72 h, and the cell viability was determined by the MTT assay. Data are expressed as mean ±S. E. of three experiments. *, P < 0.05, **, P < 0.01，vs. the control group.
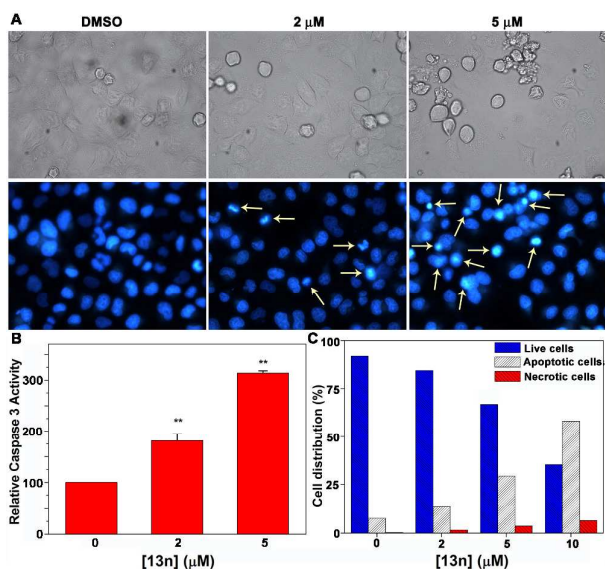
Figure 5. Induction of apoptosis by 13n. (A) Analysis of apoptosis by nuclear morphology changes. The HeLa cells were incubated with different concentrations of **13n** for 12 h followed by Hoechst 33342 staining, which showed typical apoptotic morphology changes after **13n** treatment. Phase contrast (top panel) and fluorescence (bottom panel) images were acquired by inverted fluorescence microscopy. (B) Activation of caspase 3 by **13n**. The HeLa cells were incubated with the indicated concentrations of **13n** for 12 h and the caspase 3 activity in the cell extracts was determined by a colorimetric assay. (C) Quantification of apoptosis by Annexin-V/PI double-staining assay. The HeLa cells were incubated with the indicated concentrations of **13n** for 24 h and then analysis of apoptosis by Annexin-V/PI double-staining assay.   *, $P < 0.05$, **, $P < 0.01$, vs. the control group.

1
2
3
4
5
6
7
8
9
10
11
12
13
14
15
16
17
18
19
20
21
22
23
24
25
26
27
28
29
30
31
32
33
34
35
36
37
38
39
40
41
42
43
44
45
46
47
48
49
50
51
52
53
54
55
56
57
58
59
60

TOC